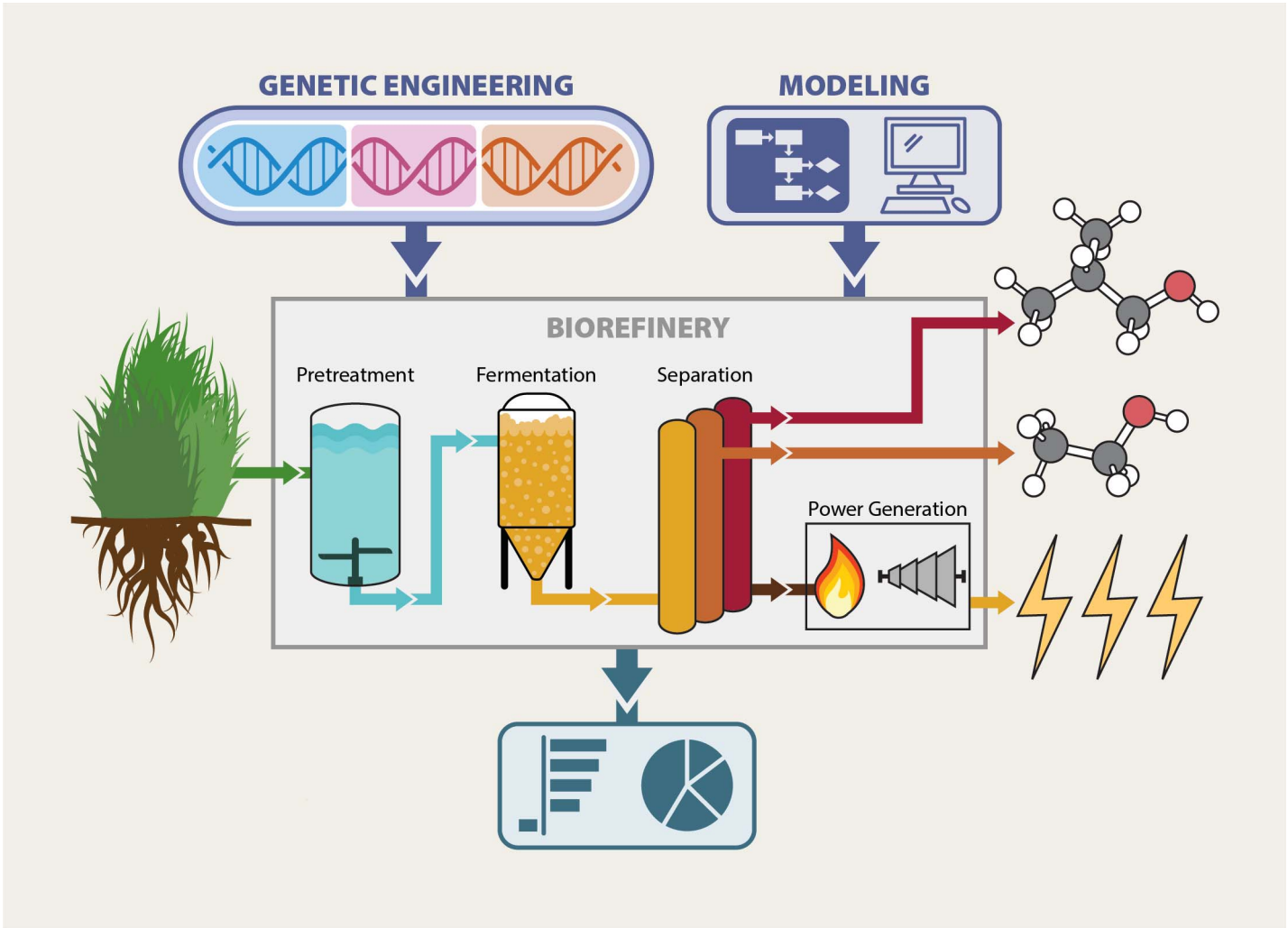

Showcasing experimental and computational research from the Great Lakes Bioenergy Research Center, United States.

High yield co-production of isobutanol and ethanol from switchgrass: experiments, and process synthesis and analysis

Here, we engineer a yeast strain and demonstrate its capability for high-yield co-production of isobutanol and ethanol from switchgrass hydrolysate. Also, based on experimental results, we design a switchgrass-to-alcohol biorefinery and analyse its performance and economic feasibility. Our analysis suggests that improvements in the hydrolysis enzyme loading and the conversion of xylose to alcohols will have the greatest economic impact. Image by Matthew Wisniewski / Wisconsin Energy Institute.

As featured in:

See Maravelias *et al.*, *Sustainable Energy Fuels*, 2023, **7**, 3266.

ROYAL SOCIETY OF CHEMISTRY

rsc.li/sustainable-energy

Registered charity number: 207890

Sustainable Energy & Fuels

ROYAL SOCIETY OF CHEMISTRY

PAPER

View Article Online
View Journal | View Issue

Check for updates

Cite this: *Sustainable Energy Fuels*, 2023, 7, 3266

High yield co-production of isobutanol and ethanol from switchgrass: experiments, and process synthesis and analysis†

Arthur E. Pastore de Lima, [ab] Russell L. Wrobel, [bc] Brandon Paul, [ab] Larry C. Anthony,[d] Trey K. Sato, [b] Yaoping Zhang, [b] Chris Todd Hittinger [bc] and Christos T. Maravelias *[ef]

Biofuels from sustainable feedstocks are a promising option for carbon-neutral bioenergy, where isobutanol has been receiving attention due to its advantageous physical and chemical properties. In this work, the production of isobutanol from carbohydrates in ammonia fiber expansion-pretreated switchgrass hydrolysate is investigated. We engineer a yeast strain by hybridizing an industrial starch isobutanologen with a strain that can tolerate the stresses of lignocellulosic hydrolysates. This strategy increases isobutanol production through ethanol co-production, which enables improved yeast growth and higher metabolic flux under these stressful conditions, likely due to the presence of at least some pyruvate decarboxylase. Furthermore, we develop a process for the recovery of isobutanol and ethanol from the broth and perform technoeconomic analysis of the switchgrass-to-alcohol biorefinery based on experiments. The yeast consumes all available glucose, but no xylose, available in the hydrolysate and co-produces isobutanol and ethanol at 23.7% and 61.8% theoretical yields, respectively. An estimated baseline minimum selling price of $11.41 per GGE for isobutanol and ethanol is determined and sensitivity analysis identified the key parameters affecting the economic feasibility of the process. Specifically, hydrolysis enzyme loading, the sugar concentration in hydrolysate, and potential fermentation technological advances, such as xylose conversion to alcohols, were shown to have the greatest economic impact.

Received 16th December 2022
Accepted 22nd May 2023

DOI: 10.1039/d2se01741e

rsc.li/sustainable-energy

Open Access Article. Published on 23 June 2023. Downloaded on 2/1/2026 3:53:11 PM.
This article is licensed under a Creative Commons Attribution-NonCommercial 3.0 Unported Licence.

1. Introduction

Isobutanol is a promising biofuel with superior properties compared to ethanol, which is currently the most used biofuel throughout the world. Isobutanol has higher energy density and lower vapor pressure than ethanol, and the vapor pressure of an isobutanol–gasoline blend is lower than gasoline. In contrast, mixing ethanol with gasoline increases the vapor pressure of the mixture over a wide range of compositions.[1] The lower oxygen content of isobutanol (21.6 wt%) compared to ethanol (34.7 wt%) allows for higher volumes of isobutanol to be blended with gasoline. Isobutanol is less susceptible to phase separation from gasoline and has lower hygroscopicity, resulting in isobutanol–gasoline blends that are less corrosive and more suitable for pipeline transportation.[2] Finally, only minor modifications to ethanol biorefineries are required to produce isobutanol.[3]

Besides its advantageous properties as a fuel, isobutanol is a suitable precursor for different chemicals, such as ketones,[4] isobutyl acetate,[5] and isobutene.[6] In particular, isobutene is a platform chemical that can be further upgraded to chemicals such as *p*-xylene,[7] methacrolein and methacrylic acid,[8] butyl rubber and other polymers,[9] isooctane, or other fuel additives, such as *tert*-butyl ethers.[10,11] Furthermore, isobutene can be oligomerized to fuel distillates in the range of jet fuel and diesel.[12–15]

One of the most important industrial processes for isobutanol production is the hydroformylation of propylene (oxo synthesis).[16] Propylene, carbon monoxide, and hydrogen react to produce a mixture of isobutyraldehyde and butyraldehyde, which are hydrogenated to isobutanol and *n*-butanol, respectively. The feedstock propylene is mainly obtained from fossil-

[a]*Department of Chemical and Biological Engineering, University of Wisconsin–Madison, 1415 Engineering Dr, Madison, WI 53706, USA*

[b]*DOE Great Lakes Bioenergy Research Center, University of Wisconsin, 1552 University Avenue, Madison, WI 53726, USA*

[c]*Laboratory of Genetics, Wisconsin Energy Institute, J. F. Crow Institute for the Study of Evolution, Center for Genomic Science Innovation, University of Wisconsin–Madison, Madison, WI 53726, USA*

[d]*IFF, Health and Biosciences, Wilmington, DE, USA*

[e]*Department of Chemical and Biological Engineering, Princeton University, Princeton, NJ 08544, USA. E-mail: maravelias@princeton.edu*

[f]*Andlinger Center for Energy and the Environment, Princeton University, Princeton, NJ 08544, USA*

† Electronic supplementary information (ESI) available. See DOI: https://doi.org/10.1039/d2se01741e

This journal is © The Royal Society of Chemistry 2023

Open Access Article. Published on 23 June 2023. Downloaded on 2/1/2026 3:53:11 PM.
This article is licensed under a Creative Commons Attribution-NonCommercial 3.0 Unported Licence.

based sources through an energy-intensive process (steam cracking of propane). An alternative means to produce isobutanol is by biological conversion of carbohydrate molecules by microbes.[17] Microbial fermentation sustainably converts sugars (*e.g.*, glucose, xylose) obtained from lignocellulosic biomass to biofuels and products.

Lignocellulosic biomass is a low-cost and largely available feedstock option. Furthermore, the use of lignocellulosic biomass avoids the use of food crops for fuel and energy production because lignocellulose does not directly compete with food production.[18] For instance, switchgrass is a lignocellulosic biomass crop that can be grown on lands that are not used for food production and requires low nitrogen input.[19]

Lignocellulosic biomass requires a pretreatment step to increase the yield of fermentable sugars. Biomass pretreatment disrupts the structure of the lignocellulosic material and exposes the carbohydrate polymers, which makes cellulose and hemicellulose more accessible to the enzymes used in the subsequent hydrolysis step.[20] Ammonia fiber expansion (AFEX) is a pretreatment that employs ammonia at high temperatures and pressure. The use of ammonia has the advantage of solubilizing lignin, which allows for the fractionation of biomass and increases the efficiency of enzymes during hydrolysis.[21] In the hydrolysis step, the enzymes convert the cellulose and hemicellulose into sugars (mainly glucose and xylose). Next, the hydrolysate is sent to fermentation, where it is inoculated with the fermenting microorganisms consuming sugars to produce alcohols.[22,23] To overcome the low tolerance of microorganisms to isobutanol, *in situ* product removal methods are required to reduce isobutanol concentration. The most promising techniques are vacuum evaporation, adsorption, pervaporation, gas stripping, and solvent extraction.[24]

Isobutanol is naturally produced *via* the Ehrlich pathway at low mg L^{-1} titers from amino acid degradation by native yeast strains, such as *Saccharomyces cerevisiae*,[25] whereas many microorganisms typically cannot produce appreciable isobutanol natively.[26] Microbial engineering has been extensively applied to enhance isobutanol production and increase the yields and titers obtained by different microorganisms, such as *S. cerevisiae*,[27–30] *Escherichia coli*,[31–33] and many others.[34–43]

Different feedstocks have been used to produce isobutanol using these microorganisms. Atsumi *et al.* engineered *E. coli* bacteria to produce 22 g L^{-1} of isobutanol from glucose.[32] Jung *et al.* produced 23 g L^{-1} of isobutanol using engineered *Enterobacter aerogenes* from sugarcane bagasse.[42] Switchgrass[39] and cellulose[37] were used to produce 0.66 g L^{-1} by *Caldicellulosiruptor bescii* and 0.17 g L^{-1} of isobutanol by *Clostridium cellulolyticum*, respectively, with no hydrolysis step. Other works focused on the consumption of hemicellulose fraction by bacterium[40] and xylose by yeast[29,44,45] to produce isobutanol, albeit at low titers and yields. Nakashima and Tamura were able to produce 11 g L^{-1} of isobutanol by *E. coli* using a medium with a mixture of glucose and xylose.[46] Note that in some systems, byproducts, such as ethanol,[43] 2-methyl-1-butanol,[29] hexanol,[39] lactate, succinate,[47] and others, are produced.

To assess the economic feasibility of new processes and microorganisms used for isobutanol production in lignocellulosic biorefineries, analyses based on experimental data must be carried out. Technoeconomic analysis of isobutanol production system has been conducted by a few authors.[3,48,49] Tao *et al.* reported an isobutanol minimum fuel selling price (MFSP) of $3.62 per gasoline gallon equivalent (GGE) using corn stover as feedstock; they considered isobutanol yields from glucose and xylose of 85% of the theoretical maximum and performed sensitivity analysis.[49] Roussos *et al.* determined an MFSP of $6.53 per GGE ($4.14 per GGE) for isobutanol using corn stover as feedstock and assuming yields of 85% (90%) of the theoretical maximum from glucose and xylose,[3] which are based on the work of Tao *et al.*[49] Note that the high xylose-to-isobutanol yields used in these works were not verified experimentally; it was assumed that xylose is converted at yields comparable to glucose. Furthermore, these works did not consider the co-production of isobutanol and other (by-) products.

In summary, many experimental works have focused on engineering microbes to produce isobutanol from different substrates. Obtaining high-yield fermentation data from lignocellulosic biomass hydrolysate is still a challenge due to the inhibitory components in the hydrolysates; the toxicity of the isobutanol product itself on microorganisms; metabolic barriers that limit biofuel titer, rate, and yield; and high water content in the broth.[24] However, producing isobutanol at high yields using lignocellulosic biomass and identifying areas of improvement are necessary to obtain an economically competitive biomass-based isobutanol. The contribution of this work is three-fold. First, we demonstrate the high-yield co-production of isobutanol and ethanol from AFEX-pretreated switchgrass hydrolysate (ASGH) by a hybrid triploid yeast strain. The isobutanologen co-produces ethanol to enable growth and metabolic flux under these stressful conditions. Second, we synthesize a switchgrass-to-alcohol biorefinery with emphasis on the separations necessary to obtain isobutanol and ethanol from the fermentation broth. Finally, we perform a technoeconomic analysis based on experimental results, thus providing an economic assessment for isobutanol and ethanol co-production in an integrated pipeline using our hybrid yeast strain. We provide further insights into the impact of potential process and fermentation strain improvements on the economics of the system using sensitivity analysis.

2. Results

2.1. Fermentation

The yHRW253 triploid yeast strain results from the hybridization of a diploid industrial isobutanologen, BTX1858 (see Section 5.1), with the haploid GLBRCY945 strain, which is genetically engineered to ferment xylose to ethanol[50] (see Section 5.1). While the BTX1858 strain lacks the pyruvate decarboxylase-encoding genes (*PDC*) that are necessary for biosynthesis of ethanol, the yHRW253 triploid contains single copies of the *PDC1*, *PDC5*, and *PDC6* genes, which are inherited from the GLBRCY945 ethanologenic parent. Similarly, the industrial isobutanologen parent has functional copies of several genes whose inactivation is required for the

Open Access Article. Published on 23 June 2023. Downloaded on 2/1/2026 3:53:11 PM. This article is licensed under a Creative Commons Attribution-NonCommercial 3.0 Unported Licence.

fermentation of xylose in the ethanologenic parent.[50] The industrial isobutanologen produces isobutanol but not ethanol in a synthetic production medium (Table S1†), but it does not grow or excrete appreciable isobutanol or ethanol in ASGH anaerobically (Table S2†). The lignocellulosic ethanologen grows well anaerobically and can produce ethanol from both glucose and xylose in ASGH (Table S3†).[50]

The major extracellular end-products obtained from the anaerobic fermentation of ASGH by yHRW253 are ethanol, isobutanol, and glycerol. The ASGH contains 56.6 g L^{-1} glucose and 39.7 g L^{-1} xylose (see Section 5.2). Table 1 shows the titer and yield from glucose for these products. Glucose is completely consumed, while xylose remains unconverted. The yield of alcohols from glucose is 85.5% ± 0.9% of the theoretical maximum, and the ratio of ethanol/isobutanol produced is 3.24 ± 0.05.

2.2. Process synthesis

We synthesize a switchgrass-based biorefinery for the co-production of isobutanol and ethanol (Fig. 1). Switchgrass is pretreated by ammonia fiber expansion (AFEX) and hydrolyzed (HYD) to convert the cellulose and hemicellulose into sugars (glucose and xylose). The hydrolysate is sent to the fermentation block (FERM), in which glucose is converted to isobutanol and ethanol following the yields obtained experimentally (Table 1). Isobutanol and ethanol in the broth are recovered in the separation block (SEP). The stream containing the residues (solids and stillage) is filtered (FILT). The stillage is sent to the wastewater treatment block (WWT), where biogas is produced from the carbon-rich residues (*i.e.*, glucose fermentation by-products and unconverted xylose). Any glucose fermentation by-product (*e.g.*, glycerol) is treated as unconverted glucose and is assumed to be processed in the WWT block. The solids are sent to the combustor and boiler (CB), where solids and biogas are combusted to produce heat. Excess heat is used for electricity production in the turbogenerator block (TBG), and the surplus of electricity is sold to the grid.

Each block in the process (see Fig. 1) consists of multiple unit operations and is characterized by cost, energy demand (*i.e.*, heat and electricity), and conversion parameters. The baseline parameter values of the AFEX and HYD blocks are calculated from the literature[23,52–56] after adjustments to account for the values of experimental operating parameters used in this work (*e.g.*, NH_3/dry biomass ratio and enzyme loading – see Sections 5.2 to 5.4). The parameter values for FILT, WWT, CB, and TBG blocks are estimated from the literature.[23,55,56]

A process simulation for the FERM and SEP blocks is developed in Aspen Plus V11 process simulator (Aspen Technology Inc.). The SEP block uses multiple distillation columns at different pressures, similar to systems such as the acetone–butanol–ethanol separation process,[51] to recover most of the isobutanol and ethanol from the broth (see Section 5.5 for details). The process simulation results are used to estimate the parameters of the process optimization model for the FERM and SEP blocks (*e.g.*, cost and energy parameters). The isobutanol and ethanol recoveries for the baseline design are 99.5% and 97.3%, respectively. The values of estimated parameters are given in the ESI.†

To synthesize the biorefinery, we use an optimization model[55,56] that includes material and energy balances across all the major blocks of the biorefinery (*e.g.*, AFEX, HYD, FERM). We minimize the cost to produce one kg of alcohol (isobutanol + ethanol). The complete mathematical formulation is detailed in the ESI.† The switchgrass is assumed to consist of 34.1% of cellulose, 27.0% of hemicellulose, and 26.4% of lignin, and it is available at \$101 Mg^{-1}.[57] The ratio of isobutanol to ethanol produced is 0.315 kg of isobutanol per kg of ethanol, and the resulting alcohol yield is 0.111 kg of alcohol per kg of switchgrass (Fig. 1).

2.3. Technoeconomic analysis

We calculate the MFSP of isobutanol and ethanol on a GGE basis, where the MFSP can be viewed as the price required so that the total revenues are equal to the total costs of the biorefinery (details on the calculation of the MFSP are given in the ESI†). The MFSP of isobutanol + ethanol obtained for the baseline design is \$11.41 per GGE, and Fig. 2 summarizes the cost contributors of the biorefinery. The HYD block is the major cost contributor (43.3% of the MFSP), followed by switchgrass purchasing (34.0%) and AFEX (10.1%).

The total estimated heat and electricity demand of the process are 15.4 and 4.9 kW h kg^{-1} of alcohol (isobutanol + ethanol), respectively, whereas a revenue of \$2.51 per GGE is obtained from the electricity surplus sold to the grid. Most of the heat is used by the SEP (59% of total heat demand) and AFEX (34.1%) blocks, while electricity is required mostly in the HYD (57.8%) and WWT (21.5%) blocks.

2.4. Sensitivity analysis

We study the effect of several parameters on the MFSP by considering changes to (A) switchgrass price, (B) AFEX reactor residence time, (C) the ratio of NH_3/dry biomass loading during AFEX, (D) enzyme loading during HYD, (E) sugar concentration in the hydrolysate, and (F) xylose conversion in FERM. In each case, we re-estimate the MFSP by solving an updated optimization model with a new set of block parameters. Note that changes in the sugar concentration in the hydrolysate (E) and the xylose conversion during FERM (F) affect the inputs to the process simulation (see Section 5.5), and thus new process simulations are performed to re-calculate the FERM and SEP

Table 1 Titers (g L^{-1}) and yields (% of theoretical maximum) for major products from glucose in AFEX-pretreated switchgrass hydrolysate (ASGH) fermented anaerobically with yHRW253 for 48 h ($N = 3$, ±s.d.)

Product	Titer (g L^{-1})	Yield (% of theoretical maximum)[a]
Isobutanol	5.52 ± 0.04	23.7% ± 0.2%
Ethanol	17.87 ± 0.25	61.8% ± 0.9%
Glycerol	5.13 ± 0.17	NC[b]

[a] The theoretical yield of isobutanol (ethanol) is 0.41 (0.51) g g^{-1} of glucose. Results based on initial glucose concentration of 56.6 g L^{-1} and xylose concentration of 39.7 g L^{-1}. [b] NC: not calculated.

 This journal is © The Royal Society of Chemistry 2023

Open Access Article. Published on 23 June 2023. Downloaded on 2/1/2026 3:53:11 PM.
This article is licensed under a Creative Commons Attribution-NonCommercial 3.0 Unported Licence.

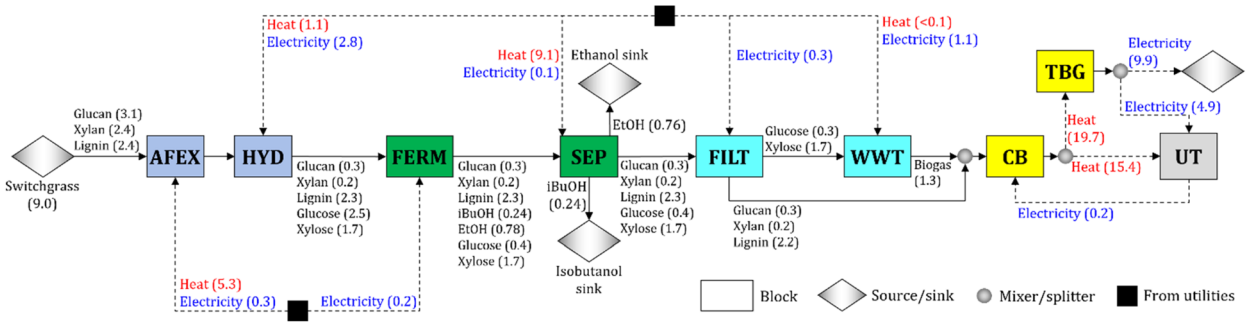

Fig. 1 Block flow diagram of the baseline switchgrass-to-alcohol biorefinery. Mass flows are in units of kg kg^{-1} of alcohol (isobutanol + ethanol) produced, and heat and electricity flows are in units of kW h kg^{-1} of alcohol. Abbreviations – AFEX: ammonia fiber expansion, CB: combustor and boiler, FERM: fermentation, FILT: filtration, HYD: hydrolysis, SEP: separations, TBG: turbogenerator, UT: utilities, WWT: wastewater treatment.

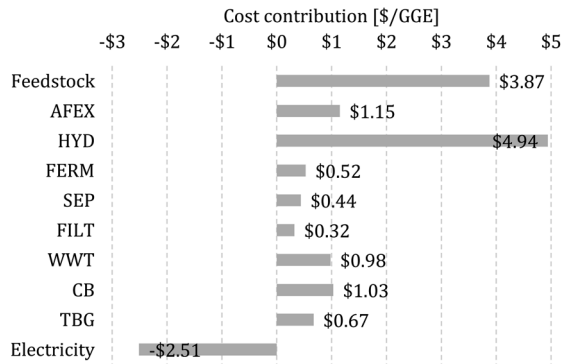

Fig. 2 Cost contributions in the baseline biorefinery. The MFSP is $11.41 per gasoline gallon equivalent (GGE).

block parameters. More details can be found in the ESI.† Fig. 3a shows the change in the MFSP (ΔMFSP) for each case. The detailed cost contributions in each case are shown in Fig. 3b.

In case (A), a 25% reduction in the switchgrass price (from $101 Mg^{-1} to $76 Mg^{-1}) reduces the feedstock cost contribution by $0.96 per GGE, representing a 8.4% MFSP decrease. In case (B), the AFEX residence time is reduced from 30 to 15 min (50%), affecting the capital and fixed operating costs, and resulting in savings of $0.29 per GGE (2.6%). In case (C), the mass ratio of NH_3/dry biomass loaded in the AFEX reactor is reduced from 1.0 to 0.5 (50%), which affects the make-up flow of ammonia, the energy demand, and the capital costs of AFEX. The MFSP is reduced by $0.75 per GGE (6.6%), due to cost savings of $0.22 per GGE and an additional $0.54 per GGE in electricity surplus revenue.

In our analysis, we assumed that hydrolysis enzymes are produced on-site[23] and that the cost and energy demand associated with enzyme production scales with enzyme loading. In case (D), the enzyme loading is reduced from 93 to 46.5 mg protein per g glucan (50% reduction), decreasing the MFSP by $2.48 per GGE (21.7%). The improvement comes from a significant reduction in HYD costs ($2.13 per GGE) and additional electricity surplus revenue ($0.35 per GGE).

In case (E), we consider a higher sugar concentration in the hydrolysate, while maintaining the same glucose/xylose ratio. The sugar concentration is increased by 50%, from 96.3 g L^{-1} to 144.5 g L^{-1} (84.9 g L^{-1} of glucose and 59.6 g L^{-1} of xylose). The cost and energy demand parameters of the FERM and SEP blocks are re-estimated using process simulation based on the new sugar concentration. The MFSP decreases by $1.38 per GGE (12.1%) due to cost savings ($0.66 per GGE) and additional electricity surplus revenue ($0.72 per GGE).

In case (F), we consider that the yeast would be capable of converting xylose to isobutanol and ethanol (*e.g.*, through

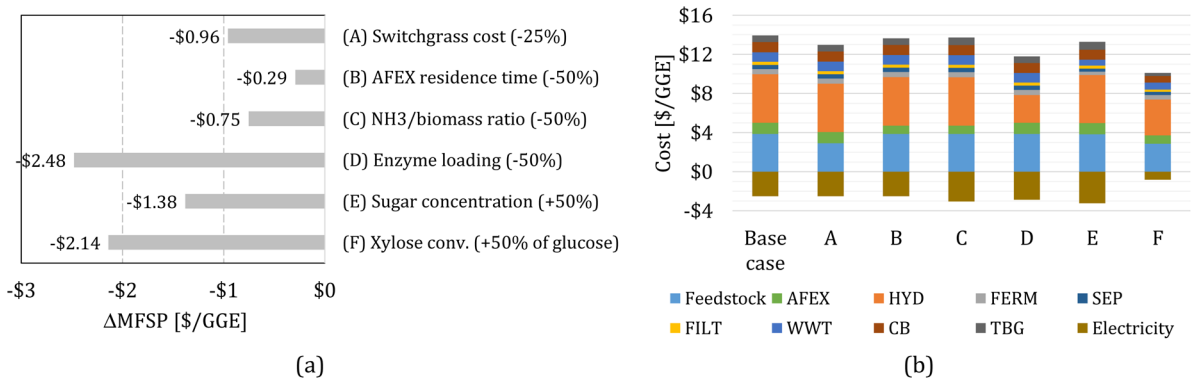

Fig. 3 (a) Change in the minimum fuel selling price (ΔMFSP) for each case. The baseline MFPS is $11.41 per GGE. (b) Cost contributions in the switchgrass-to-alcohol biorefinery for cases (A) to (F).

Open Access Article. Published on 23 June 2023. Downloaded on 2/1/2026 3:53:11 PM.
This article is licensed under a Creative Commons Attribution-NonCommercial 3.0 Unported Licence.

further engineering of yHRW253), achieving half the glucose yields (*i.e.*, the yields to isobutanol and ethanol from xylose are 11.8% and 30.9% of the theoretical maximum, respectively). As before, the cost and energy demand parameters for the FERM and SEP blocks are re-calculated. The MFSP decreases by \$2.14 per GGE (18.7%). Note that revenues from electricity surplus are reduced by 67%, representing \$1.69 per GGE of lost revenue compared to the baseline design; however, cost savings of \$3.83 per GGE are achieved by all blocks throughout the biorefinery.

Finally, we perform sensitivity analysis considering multiple changes simultaneously. First, we consider simultaneous improvements in the AFEX and HYD bocks, combining cases (B), (C), and (D). Second, we consider improvements in switchgrass purchasing cost and the FERM block, combining cases (A), (E), and (F). Finally, we consider all improvements, (A) through (F), simultaneously. The change in MFSP and cost contributions for the combined cases are shown in Fig. 4.

The improvements in AFEX and HYD, cases (B)–(D), reduce the MFSP by \$3.45 per GGE (30.3%); electricity revenue increases by \$0.89 per GGE and costs decrease by \$2.56 per GGE, mainly in the AFEX and HYD blocks. The improvements in FERM combined with switchgrass cost reduction, cases (A), (E), and (F), decrease the MFSP by \$3.95 per GGE (34.6%), where \$1.16 per GGE of electricity surplus revenue is lost due to reduced heat production from biogas, but cost reductions amount to \$5.11 per GGE.

Finally, the combination of all improvements considered in this work results in an MFSP of \$4.94 per GGE (a reduction of \$6.47 per GGE compared to the baseline design). The reduction in the MFSP is mainly due to cost savings (\$6.97 per GGE), whereas the electricity surplus revenue drops by \$0.51 per GGE.

3. Discussion

3.1. Hybrids maintain hydrolysate tolerance and isobutanol production, while co-producing ethanol

Here we hybridize an industrial starch isobutanologen that could not tolerate AFEX-switchgrass hydrolysate with a stress-tolerant, xylose-fermenting ethanologen. The triploid hybrid strain grows in the hydrolysate and co-produces isobutanol and ethanol at high yields from glucose. Some of this improved performance likely stems from dominant alleles in the innate stress tolerance of the genetic background chosen for the xylose-fermenting ethanologen.[58] The functional copies of *PDC* introduced by this genetic background also may play a role in improving flux and redox balance, likely due to the dominance of the *PDC* alleles. This genetic background also has four gene deletions that are required for optimized conversion of xylose to ethanol,[50] and these deletions are presumably recessive to functional copies introduced by industrial isobutanologen. Technoeconomic analysis suggests that one of the top targets for future improvement should be to optimize xylose fermentation, such as by eliminating the functional copies of these four genes in the hybrid or similar strains.

3.2. Technoeconomic analysis

We estimate the MFSP for a baseline design of a lignocellulosic biorefinery co-producing isobutanol and ethanol using the yHRW253 hybrid strain, while our sensitivity analysis seeks to provide insights into the impact of technological improvements. The MFSP can be reduced by more than \$1 per GGE if a 50% improvement is achieved in any of the following parameters: hydrolysis enzyme loading, sugar concentration in hydrolysate, or xylose conversion (Fig. 3a).

We consider improvements in the AFEX and HYD blocks by reducing the NH_3/dry biomass mass ratio, the AFEX residence time, and the enzyme loading by 50% compared to the baseline design. Note that similar, and even more optimistic, improvements have been considered in other works. For example, Teymouri *et al.* reported an optimal AFEX residence time of 5 min (83.3% lower compared to this work) for corn stover pretreatment.[59] Humbird *et al.* considered an enzyme loading of 20 mg of protein per g of glucan in a biorefinery for bioethanol production (*i.e.*, 78.5% lower).[23] Our results show that the MFSP can be reduced by \$3.45 per GGE with the 50% improvements considered in the AFEX and HYD. Therefore, a lower NH_3/biomass ratio in AFEX pretreatment and lower enzyme loading in HYD can lead to improved process economics.

The sensitivity analysis shows that the sugar concentration in the hydrolysate and the ability to convert xylose to alcohols

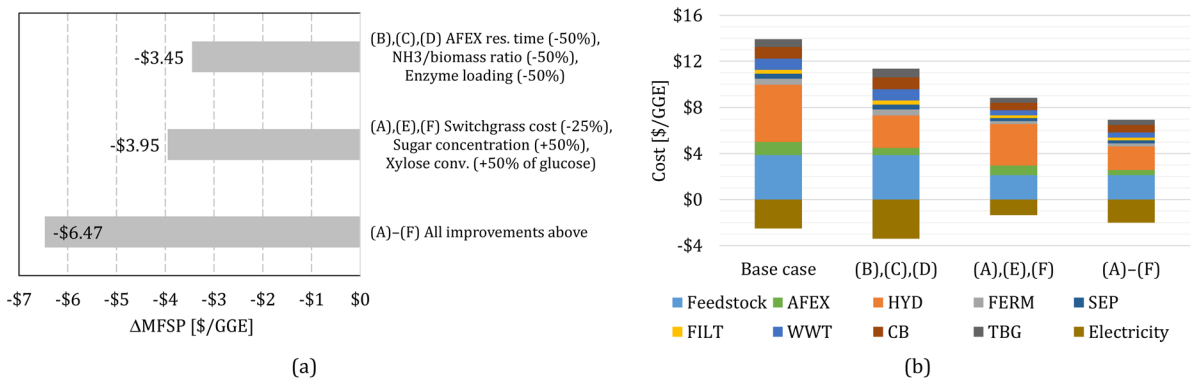

Fig. 4 (a) Change in MFSP based on multiple improvements. (b) Cost contributions in the switchgrass-to-alcohol biorefinery for scenarios with multiple improvements.

 This journal is © The Royal Society of Chemistry 2023

Open Access Article. Published on 23 June 2023. Downloaded on 2/1/2026 3:53:11 PM.
This article is licensed under a Creative Commons Attribution-NonCommercial 3.0 Unported Licence.

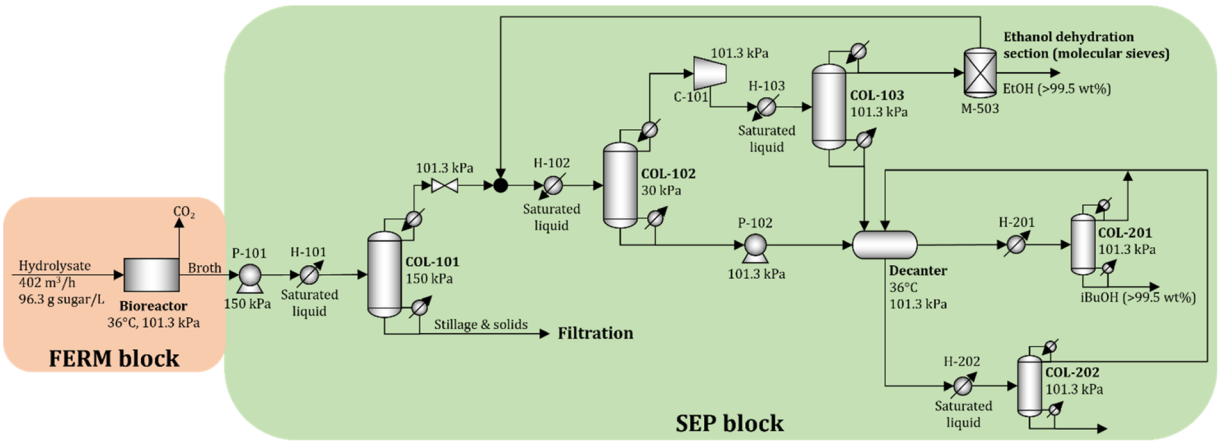

Fig. 5 Process flow diagram of the baseline FERM and SEP blocks simulated in Aspen Plus V11.

are important drivers of the MFSP. Higher sugar concentration in the hydrolysate reduces the volume of broth required to be processed (to produce a fixed amount of alcohol), thereby reducing the size of equipment required in FERM and SEP blocks and generating less volume of wastewater to be treated; it also decreases the heat required in the SEP block, increasing the surplus of electricity sold to the grid (Fig. 3b).

The fermentation of xylose reduces the unit costs ($ per kg of alcohol) of all biorefinery blocks due to higher product yields (Fig. 3b). In case (F), and combined cases [(A), (E) and (F)] and [(A)–(F)], the conversion of xylose to alcohols results in smaller sugar amounts (and switchgrass, consequently) required to produce the same amount of alcohol, thereby reducing the flows and unit costs throughout the biorefinery. Note that unconverted xylose generates biogas in the WWT block (Fig. 1), resulting in a significant decrease in electricity surplus once a fraction of xylose is converted to alcohols in FERM (Fig. 3b). Therefore, further engineering of yeast yHRW253 towards xylose fermentation to increase product yields will result in significant cost reduction.

Note that both sugar concentration in hydrolysate and xylose conversion affect the concentration of isobutanol in the broth. In the sensitivity analysis, we assumed that microorganisms would not be significantly affected by the higher isobutanol concentration compared to the baseline design. This assumption may not hold at higher isobutanol yields, but strategies to remove isobutanol-rich vapors directly from the broth (*e.g.*, vacuum stripping) could address this potential limitation.

Finally, we note that other improvements, not considered herein (*e.g.*, the use of simultaneous saccharification and fermentation) could also lead to better process economics.

4. Conclusions

We study a system co-producing, at high yields, isobutanol and ethanol from glucose in switchgrass hydrolysate pretreated by AFEX. We employ a novel yeast strain derived from the hybridization of an industrial starch-to-isobutanol strain (BTX1858), which does not ferment in ASGH, with a xylose-fermenting, stress-tolerant strain (GLBRCY945) that does not produce isobutanol. The resulting yHRW253 hybrid strain consumes all glucose, with an 85.5% theoretical yield of isobutanol and ethanol. Xylose remains unconverted, likely due to complementation of the loss-of-function genetic modifications in the GLBRCY945 strain that enable xylose fermentation.[50]

We synthesize a switchgrass-to-alcohol biorefinery using the yHRW253 hybrid strain for isobutanol and ethanol co-production for $11.41 per GGE. Cost analysis of the baseline design shows that the major biorefinery costs are HYD operation followed by switchgrass purchasing. Furthermore, we identify critical parameters that impact the economic feasibility of the proposed biorefinery. Our results suggest that the effect of lower NH_3/biomass mass ratio during AFEX pretreatment and lower enzyme loading during HYD should be studied to ensure high sugar yields, while avoiding large economic burdens to the biorefinery. In addition, further research focused on converting the available xylose to alcohols is critical to reducing the switchgrass cost contribution and obtaining a more economically competitive biorefinery.

5. Methods

5.1. Yeast strain engineering

The GLBRCY945 strain is an ethanologen derived from the stress-tolerant, xylose-fermenting GLBRCY560 yeast strain described previously[50,60] with one additional genetic modification. The GLBRCY560 strain contains a series of genetic modifications that enable anaerobic xylose fermentation to ethanol. These modifications include integration of a DNA cassette that allows over-expression of xylose isomerase, xylulokinase, and the *TAL1* gene, as well as deletion mutations in *GRE3*, *HOG1*, *IRA2*, and *ISU1* genes. In GLBRCY945, the *FLO8* gene was deleted by replacement with the *hphMX* marker by homologous recombination. Deletion of *FLO8* was verified by Polymerase Chain Reaction (PCR) and Sanger sequencing.

The industrial isobutanologen BTX1858 was obtained from Butamax Advanced Biofuels LLC, under a Material Transfer Agreement. The BTX1858 strain produces isobutanol as a single

Open Access Article. Published on 23 June 2023. Downloaded on 2/1/2026 3:53:11 PM. This article is licensed under a Creative Commons Attribution-NonCommercial 3.0 Unported Licence.

alcohol at high yield. The GLBRCY945 and BTX1858 strains were transformed with the HyPr plasmids pHRW34 and pHCT2, respectively, and mating was induced as described previously.[61,62] Hybrids were selected YPD plates containing 100 mg mL^{-1} of both nourseothricin and zeocin. The HyPr plasmids were cured from the triploid hybrid by growing for multiple generations in non-selective liquid media. The yHRW253 hybrid was verified by the PCR amplification of the polymorphic loci *FLO8*, *GRE3*, and *HOG1*.

5.2. Switchgrass pretreatment and enzymatic hydrolysis

The milled and AFEX-pretreated year-2016 switchgrass was used as the lignocellulosic biomass feedstock for enzymatic hydrolysis to obtain the sugars from the biomass, as described previously.[63] The mass fraction of major components in the untreated year-2016 switchgrass was determined using the NREL Laboratory Analytical Procedure:[64] 0.341 ± 0.004 glucan; 0.216 ± 0.005 xylan; 0.016 ± 0.001 galactan; 0.029 ± 0.032 arabinan; 0.206 ± 0.015 acid-insoluble lignin; and unknown ash. The switchgrass was loaded with ammonia at a 1 g NH_3 per g of dry biomass ratio. The pretreatment was carried out at 100 ± 10 °C for 30 min. Hydrolysis was conducted at 7% of glucan loading, using an enzyme loading of approximately 93 mg protein per g glucan. The hydrolysis was carried out at 50 °C for 7 days and the resulting ASGH contains 56.6 g L^{-1} glucose and 39.7 g L^{-1} xylose.

5.3. Fermentations

The fermentation experiment in Table 1 was carried out in a respirometer system as described previously,[65] with the following modifications. The starter cultures were grown in YPD aerobically overnight and then inoculated into 4 mL of each hydrolysate in sterile 60 mL Wheaton serum bottles with initial OD_{600} values of 0.5. After capping them with blue butyl 20 mm rubber stoppers, bottles were degassed and flushed with pure N_2 gas in a manifold system at least three times. Finally, bottles were filled with N_2 gas and then connected to respirometer cartridges. The volumes of gas (mainly CO_2) produced by the growing culture were recorded every 10 min during 48 h fermentations. At the end of the fermentations, the end products were collected and analyzed by HPLC-RID and GC/MS for sugar, ethanol, and isobutanol concentrations as described previously.[27] Final cell density OD_{600} measurements were made with a Shimadzu UV-1280 spectrophotometer. Percent theoretical yields were calculated using the amount of glucose consumed.

The bioreactor fermentations in Tables S1–S3† were conducted for 48 hours in 250 mL Minibio bioreactors (Applikon Biotechnology, Foster City, CA) containing 100 mL of ASGH or production medium (1.7 g L^{-1} Difco Yeast Nitrogen Base without Amino Acids and Ammonium Sulfate, 5 g L^{-1} ammonium sulfate, 1 g L^{-1} yeast extract, 60 g L^{-1} dextrose, 2 mL L^{-1} 1 : 100 diluted Antifoam 204, 3 mL L^{-1} nicotinic acid (10 mg mL^{-1} stock), 3 mL L^{-1} thiamine (10 mg mL^{-1} stock), 0.8 g L^{-1} KH_2PO_4, 1.9 g L^{-1} K_2HPO_4, pH 5.2, 0.2 μm filter-sterilized). Prior to fermentation, ASGH was adjusted to pH 5.8 using 10 N NaOH and filtered through a 0.2 μm filter to remove precipitates and ensure sterility. Overnight aerobic-grown starter cultures of Y945 in YPD (10 g L^{-1} yeast extract, 20 g L^{-1} peptone, 20 g L^{-1} dextrose) and BTX1858 in SD (19.5 g L^{-1} MES, 1.7 g L^{-1} Difco Yeast Nitrogen Base without Amino Acids and Ammonium Sulfate, 5 g L^{-1} ammonium sulfate, 1.7 g L^{-1} yeast drop-out mix without uracil, 3 g L^{-1} glucose, pH 5.5 using 5% KOH, 0.2 μm filter-sterilized) were centrifuged at 14 000*g* for 3 minutes, and the supernatants were discarded. The cell pellets were resuspended into 5 mL of ASGH or production medium from each vessel, and the suspensions were then inoculated back into each vessel to give each an initial OD_{600} of 0.5. Fermentation was conducted at 30 °C with continuous stirring (500 rpm), pH was controlled at 5.8, and samples were removed from the bioreactors for an OD_{600} measurement to monitor cell growth and for HPLC-RID and GC/MS to measure the concentrations of glucose, xylose, and the end products as described previously.[27] Percent theoretical yields were calculated using the amount of glucose (and xylose for GLBRCY945) consumed.

5.4. Process optimization model

The optimization model of the switchgrass-to-alcohol biorefinery (Fig. 1) is formulated in GAMS (36.1.0). The objective is to minimize the cost to produce a kg of alcohol (isobutanol + ethanol). Each block is described by cost, energy demand, and conversion parameters, describing, respectively, the cost, and heat and electricity requirements of the unit operations associated with the block. The conversion parameters describe the conversion of components in the inlet stream into components in the outlet streams of the block. The complete mathematical formulation is presented in the ESI.†

The cost and energy demand parameters for the AFEX block are adapted from the literature[52] after adjusting for the NH_3/dry biomass mass ratio and residence time used in this study (see Section 5.2). The cost and energy demand parameters of the HYD block are estimated from NREL reports[53,54] and include on-site enzyme production,[23] which is scaled based on the enzyme loading of this study. Linear scaling is used for material and energy flows, while power-law scaling (exponent of 2/3) is used for capital costs. We estimate the cost and energy demand parameters for the FERM and SEP blocks using detailed process simulations (Section 5.5) due to the dependence of these parameters on the product yields and ASGH sugar concentration. The parameters for FILT, WWT, CB, and TBG blocks are estimated from the literature.[23,55,56] The list of used parameter values is detailed in the ESI.†

5.5. Process simulation

To obtain accurate estimates of the cost and energy demand of the FERM and SEP blocks, the unit operations of these blocks are simulated using Aspen Plus V11 (Aspen Technology Inc.) for a biorefinery processing 2000 Mg d^{-1} of dry biomass. The process flow diagram is shown in Fig. 5.

A total of 402 m^3 h^{-1} of hydrolysate is processed in 12 parallel bioreactors (each processing 33.5 m^3 h^{-1} of hydrolysate). Since the titer of isobutanol in the fermentation broth is

 This journal is © The Royal Society of Chemistry 2023

Open Access Article. Published on 23 June 2023. Downloaded on 2/1/2026 3:53:11 PM. This article is licensed under a Creative Commons Attribution-NonCommercial 3.0 Unported Licence.

relatively low (see Section 2.2), we consider that the concentration of isobutanol in the broth does not reach toxic levels. The broth is sent to the beer column (COL-101) operated at 150 kPa. Solids and the stillage containing large amounts of water are removed at the bottom, while the distillate, containing isobutanol, ethanol, and water, is sent to a vacuum distillation column (COL-102) operated at 30 kPa. The objective of column COL-102 (and COL-103) is to concentrate and recover most of the ethanol in the distillate stream. The distillate in COL-103 is close to the water–ethanol azeotrope, so molecular sieves (M-503) are used to dehydrate the ethanol to 99.5 wt%.[23] The bottom streams from COL-102 and COL-103 are rich in water and isobutanol, which form a heteroazeotrope. The streams are sent to a decanter to obtain two liquid phases. The water-rich phase is sent to COL-202, where water is removed at the bottom with minimal loss of isobutanol, and the distillate is recycled to the decanter. The isobutanol-rich phase is purified in COL-201 to obtain 99.5 wt% isobutanol at the bottom, and the distillate, which contains water and isobutanol, is recycled to the decanter. The details of the economic assumptions and cost and energy demand estimates are given in the ESI.†

Author contributions

AEPL: conceptualization, data curation, formal analysis, investigation, methodology, resources, software, validation, visualization, writing – original draft, writing – review & editing. RLW: conceptualization, data curation, investigation, methodology, resources, validation, writing – review & editing. BP: conceptualization, formal analysis, methodology, resources, software. LA: resources, writing – review & editing. TKS: conceptualization, formal analysis, data curation, investigation, methodology, resources, funding acquisition, validation, writing – review & editing. YZ: conceptualization, data curation, investigation, methodology, resources, funding acquisition, validation, writing – review & editing. CTH: conceptualization, formal analysis, funding acquisition, investigation, methodology, project administration, supervision, validation, writing – review & editing. CTM: conceptualization, formal analysis, funding acquisition, investigation, methodology, project administration, supervision, validation, writing – review & editing.

Conflicts of interest

Strain BTX1858 is a proprietary strain made available to researchers under a Material Transfer Agreement with Butamax Advanced Biofuels LLC, who retains all rights to the strain. LA is an employee of IFF and formerly of Butamax Advanced Biofuels LLC. TKS is an inventor on a patent that covers the genetic modifications made in the GLBRCY945 strain. CTH is an inventor on a patent application that covers the HyPr technology.

Acknowledgements

We thank Jose Serate, Dan Xie, and Evan Handowski for hydrolysate production and fermentation work; Mick McGee and the GLBRC Metabolomics Facility for HPLC-RID and Gas Chromatography analyses; and Butamax and DuPont R&D for designing and providing the industrial strain BTX1858. This work was funded by the DOE Great Lakes Bioenergy Research Center (DOE BER Office of Science DE–SC0018409). Research in the Hittinger Lab is also supported by the National Science Foundation under Grant No. DEB-1442148 and DEB-2110403, the USDA National Institute of Food and Agriculture (Hatch Project 1020204), and an H. I. Romnes Faculty Fellowship, supported by the Office of the Vice Chancellor for Research and Graduate Education with funding from the Wisconsin Alumni Research Foundation. AFEX is a trademark of MBI International (Lansing, MI).

References

1 V. F. Andersen, J. E. Anderson, T. J. Wallington, S. A. Mueller and O. J. Nielsen, *Energy Fuels*, 2010, **24**, 3647–3654.
2 D. R. Nielsen, E. Leonard, S. H. Yoon, H. C. Tseng, C. Yuan and K. L. J. Prather, *Metab. Eng.*, 2009, **11**, 262–273.
3 A. Roussos, N. Misailidis, A. Koulouris, F. Zimbardi and D. Petrides, *Processes*, 2019, **7**, 667.
4 K. Breitkreuz, A. Menne and A. Kraft, *Biofuels, Bioprod. Biorefin.*, 2014, **8**, 504–515.
5 R. Muñoz, J. B. Montón, M. C. Burguet and J. de la Torre, *Sep. Purif. Technol.*, 2006, **50**, 175–183.
6 J. D. Taylor, M. M. Jenni and M. W. Peters, *Top. Catal.*, 2010, **53**, 1224–1230.
7 Z. Lin, V. Nikolakis and M. Ierapetritou, *Ind. Eng. Chem. Res.*, 2014, **53**, 10688–10699.
8 J. Guan, C. Xu, Z. Wang, Y. Yang, B. Liu, F. Shang, Y. Shao and Q. Kan, *Catal. Lett.*, 2008, **124**, 428–433.
9 A. A. Gronowski, *J. Appl. Polym. Sci.*, 2003, **87**, 2360–2364.
10 A. Rehfinger and U. Hoffmann, *Chem. Eng. Sci.*, 1990, **45**, 1605–1617.
11 M. Sutter, E. Da Silva, N. Duguet, Y. Raoul, E. Métay and M. Lemaire, *Chem. Rev.*, 2015, **115**, 8609–8651.
12 J.-M. Restrepo-Flórez, J. Ryu, D. Witkowski, D. A. Rothamer and C. T. Maravelias, *Energy Environ. Sci.*, 2022, **15**, 4376–4388.
13 J. M. Restrepo-Flórez and C. T. Maravelias, *Energy Environ. Sci.*, 2021, **14**, 493–506.
14 M. C. Al-Kinany, S. A. Al-Drees, H. A. Al-Megren, S. M. Alshihri, E. A. Alghilan, F. A. Al-Shehri, A. S. Al-Hamdan, A. J. Alghamdi and S. D. Al-Dress, *Appl. Petrochem. Res.*, 2019, **9**, 35–45.
15 A. V. Lavrenov, T. R. Karpova, E. A. Buluchevskii and E. N. Bogdanets, *Catal. Ind.*, 2016, **8**, 316–327.
16 H.-D. Hahn, G. Dämbkes, N. Rupprich, H. Bahl and G. D. Frey, in *Ullmann's Encyclopedia of Industrial Chemistry*, Wiley-VCH Verlag GmbH & Co. KGaA, Weinheim, Germany, 2013.
17 K. K. Hong and J. Nielsen, *Cell. Mol. Life Sci.*, 2012, **69**, 2671–2690.
18 P. P. Peralta-Yahya, F. Zhang, S. B. Del Cardayre and J. D. Keasling, *Nature*, 2012, **488**(7411), 320–328.

Open Access Article. Published on 23 June 2023. Downloaded on 2/1/2026 3:53:11 PM. This article is licensed under a Creative Commons Attribution-NonCommercial 3.0 Unported Licence.

19 D. R. Keshwani and J. J. Cheng, *Bioresour. Technol.*, 2009, **100**, 1515–1523.
20 N. Mosier, C. Wyman, B. Dale, R. Elander, Y. Y. Lee, M. Holtzapple and M. Ladisch, *Bioresour. Technol.*, 2005, **96**, 673–686.
21 T. H. Kim, R. Gupta and Y. Y. Lee, in *Biofuels: Methods and Protocols*, ed. J. R. Mielenz, Humana Press, Totowa, NJ, 2009, pp. 79–91.
22 C. Ryan, *An Overview of Gevo's Biobased Isobutanol Production Process*, 2019.
23 D. Humbird, R. Davis, L. Tao, C. Kinchin, D. Hsu, A. Aden, P. Schoen, J. Lukas, B. Olthof, M. Worley, D. Sexton and D. Dudgeon, *Process Design and Economics for Conversion of Lignocellulosic Biomass to Ethanol*, 2011.
24 C. Fu, Z. Li, C. Jia, W. Zhang, Y. Zhang, C. Yi and S. Xie, *Energy Convers. Manage.: X*, 2021, **10**, 100059.
25 P. Giudici, P. Romano and C. Zambonelli, *Can. J. Microbiol.*, 1990, **36**, 61–64.
26 N. M. Lakshmi, P. Binod, R. Sindhu, M. K. Awasthi and A. Pandey, *Bioengineered*, 2021, **12**, 12308–12321.
27 F. V. Gambacorta, E. R. Wagner, T. B. Jacobson, M. Tremaine, L. K. Muehlbauer, M. A. McGee, J. J. Baerwald, R. L. Wrobel, J. F. Wolters, M. Place, J. J. Dietrich, D. Xie, J. Serate, S. Gajbhiye, L. Liu, M. Vang-Smith, J. J. Coon, Y. Zhang, A. P. Gasch, D. Amador-Noguez, C. T. Hittinger, T. K. Sato and B. F. Pfleger, *Synth. Syst. Biotechnol.*, 2022, **7**, 738–749.
28 X. Chen, K. F. Nielsen, I. Borodina, M. C. Kielland-Brandt and K. Karhumaa, *Biotechnol. Biofuels*, 2011, **4**, 1–12.
29 Y. Zhang, S. Lane, J. M. Chen, S. K. Hammer, J. Luttinger, L. Yang, Y. S. Jin and J. L. Avalos, *Biotechnol. Biofuels*, 2019, **12**, 1–15.
30 F. Matsuda, J. Ishii, T. Kondo, K. Ida, H. Tezuka and A. Kondo, *Microb. Cell Fact.*, 2013, **12**, 119.
31 I. N. Ghosh, J. Martien, A. S. Hebert, Y. Zhang, J. J. Coon, D. Amador-Noguez and R. Landick, *Metab. Eng.*, 2019, **52**, 324–340.
32 S. Atsumi, T. Hanai and J. C. Liao, *Nature*, 2008, **451**, 86–89.
33 R. Liu, F. Zhu, L. Lu, A. Fu, J. Lu, Z. Deng and T. Liu, *Metab. Eng.*, 2014, **22**, 10–21.
34 Y. Liu, I. N. Ghosh, J. Martien, Y. Zhang, D. Amador-Noguez and R. Landick, *Metab. Eng.*, 2020, **61**, 261–274.
35 M. Qiu, W. Shen, X. Yan, Q. He, D. Cai, S. Chen, H. Wei, E. P. Knoshaug, M. Zhang, M. E. Himmel and S. Yang, *Biotechnol. Biofuels*, 2020, **13**, 1–14.
36 W. Siripong, P. Wolf, T. P. Kusumoputri, J. J. Downes, K. Kocharin, S. Tanapongpipat and W. Runguphan, *Biotechnol. Biofuels*, 2018, **11**, 1–16.
37 W. Higashide, Y. Li, Y. Yang and J. C. Liao, *Appl. Environ. Microbiol.*, 2011, **77**, 2727–2733.
38 P. P. Lin, L. Mi, A. H. Morioka, K. M. Yoshino, S. Konishi, S. C. Xu, B. A. Papanek, L. A. Riley, A. M. Guss and J. C. Liao, *Metab. Eng.*, 2015, **31**, 44–52.
39 G. M. Rubinstein, G. L. Lipscomb, A. M. Williams-Rhaesa, G. J. Schut, R. M. Kelly and M. W. W. Adams, *J. Ind. Microbiol. Biotechnol.*, 2020, **47**, 585–597.
40 J. Lange, F. Müller, R. Takors and B. Blombach, *Microb. Biotechnol.*, 2018, **11**, 257–263.
41 A. Hussain, U. Shahbaz, S. Khan, S. Basharat, K. Ahmad, F. Khan and X. Xia, *BioEnergy Res.*, 2022, **1**, 1–18.
42 H. M. Jung, J. Y. Lee, J. H. Lee and M. K. Oh, *Bioresour. Technol.*, 2018, **259**, 373–380.
43 Y. Su, W. Zhang, A. Zhang and W. Shao, *Appl. Sci.*, 2020, **10**, 8222.
44 D. Brat and E. Boles, *FEMS Yeast Res.*, 2013, **13**, 241–244.
45 S. Lane, Y. Zhang, E. J. Yun, L. Ziolkowski, G. Zhang, Y. S. Jin and J. L. Avalos, *Biotechnol. Bioeng.*, 2020, **117**, 372–381.
46 N. Nakashima and T. Tamura, *J. Biosci. Bioeng.*, 2012, **114**, 38–44.
47 B. Blombach, T. Riester, S. Wieschalka, C. Ziert, J. W. Youn, V. F. Wendisch and B. J. Eikmanns, *Appl. Environ. Microbiol.*, 2011, **77**, 3300–3310.
48 H. Cai, J. Markham, S. Jones, P. T. Benavides, J. B. Dunn, M. Biddy, L. Tao, P. Lamers and S. Phillips, *ACS Sustainable Chem. Eng.*, 2018, **6**, 8790–8800.
49 L. Tao, E. C. D. Tan, R. Mccormick, M. Zhang, A. Aden, X. He and B. T. Zigler, *Biofuels, Bioprod. Biorefin.*, 2014, **8**, 30–48.
50 T. K. Sato, M. Tremaine, L. S. Parreiras, A. S. Hebert, K. S. Myers, A. J. Higbee, M. Sardi, S. J. McIlwain, I. M. Ong, R. J. Breuer, R. Avanasi Narasimhan, M. A. McGee, Q. Dickinson, A. La Reau, D. Xie, M. Tian, J. L. Reed, Y. Zhang, J. J. Coon, C. T. Hittinger, A. P. Gasch and R. Landick, *PLoS Genet.*, 2016, **12**, e1006372.
51 A. P. Mariano, M. J. Keshtkar, D. I. P. Atala, F. M. Filho, M. R. W. MacIel, R. M. I. Filho and P. Stuart, *Energy Fuels*, 2011, **25**, 2347–2355.
52 M. Laser, H. Jin, K. Jayawardhana and L. R. Lynd, *Biofuels, Bioprod. Biorefin.*, 2009, **3**, 195–218.
53 A. Aden, M. Ruth, K. Ibsen, J. Jechura, K. Neeves, J. Sheehan, B. Wallace, L. Montague, A. Slayton and J. Lukas, *Lignocellulosic Biomass to Ethanol Process Design and Economics Utilizing Co-current Dilute Acid Prehydrolysis and Enzymatic Hydrolysis for Corn Stover*, Golden, Colorado, 2002.
54 F. K. Kazi, J. Fortman, R. Anex, G. Kothandaraman, D. Hsu, A. Aden and A. Dutta, *Techno-Economic Analysis of Biochemical Scenarios for Production of Cellulosic Ethanol Techno-Economic Analysis of Biochemical Scenarios for Production of Cellulosic Ethanol*, Golden, Colorado, 2010.
55 K. Huang, P. Fasahati and C. T. Maravelias, *iScience*, 2020, **23**, 100751.
56 R. T. L. Ng, P. Fasahati, K. Huang and C. T. Maravelias, *Appl. Energy*, 2019, **241**, 491–503.
57 C. H. Geissler and C. T. Maravelias, *Appl. Energy*, 2021, **302**, 117539.
58 S. J. McIlwain, D. Peris, M. Sardi, O. V. Moskvin, F. Zhan, K. S. Myers, N. M. Riley, A. Buzzell, L. S. Parreiras, I. M. Ong, R. Landick, J. J. Coon, A. P. Gasch, T. K. Sato and C. T. Hittinger, *G3: Genes, Genomes, Genet.*, 2016, **6**, 1757–1766.
59 F. Teymouri, L. Laureano-Perez, H. Alizadeh and B. E. Dale, *Bioresour. Technol.*, 2005, **96**, 2014–2018.

 This journal is © The Royal Society of Chemistry 2023

Open Access Article. Published on 23 June 2023. Downloaded on 2/1/2026 3:53:11 PM.
This article is licensed under a Creative Commons Attribution-NonCommercial 3.0 Unported Licence.

60 S. B. Lee, M. Tremaine, M. Place, L. Liu, A. Pier, D. J. Krause, D. Xie, Y. Zhang, R. Landick, A. P. Gasch, C. T. Hittinger and T. K. Sato, *Metab. Eng.*, 2021, **68**, 119–130.
61 D. Peris, W. G. Alexander, K. J. Fisher, R. V. Moriarty, M. G. Basuino, E. J. Ubbelohde, R. L. Wrobel and C. T. Hittinger, *Nat. Commun.*, 2020, **111**(11), 1–11.
62 W. G. Alexander, D. Peris, B. T. Pfannenstiel, D. A. Opulente, M. Kuang and C. T. Hittinger, *Fungal Genet. Biol.*, 2016, **89**, 10–17.
63 Y. Zhang, J. Serate, D. Xie, S. Gajbhiye, P. Kulzer, G. Sanford, J. D. Russell, M. McGee, C. Foster, J. J. Coon, R. Landick and T. K. Sato, *Bioresour. Technol. Rep.*, 2020, **11**, 100517.
64 A. Sluiter, B. Hames, R. Ruiz, C. Scarlata, J. Sluiter, D. Templeton, and D. Crocker, *Determination of Structural Carbohydrates and Lignin in Biomass*, 2012.
65 M. Chandrasekar, L. Joshi, K. Krieg, S. Chipkar, E. Burke, D. J. Debrauske, K. D. Thelen, T. K. Sato and R. G. Ong, *Biotechnol. Biofuels*, 2021, **14**, 1–17.